Published OnlineFirst June 2, 2016; DOI: 10.1158/1541-7786.MCR-16-0068

Genomics

Molecular Cancer Research

Evolution of Dermatofibrosarcoma Protuberans to DFSP-Derived Fibrosarcoma: An Event Marked by Epithelial–Mesenchymal Transition–like Process and 22q Loss

Silvia Stacchiotti[1], Annalisa Astolfi[2], Alessandro Gronchi[3], Andrea Fontana[3], Maria A. Pantaleo[4], Tiziana Negri[5], Monica Brenca[6], Marcella Tazzari[7], Milena Urbini[2], Valentina Indio[2], Chiara Colombo[3], Stefano Radaelli[3], Silvia Brich[5], Angelo P. Dei Tos[8], Paolo G. Casali[1], Chiara Castelli[7], Gian Paolo Dagrada[5], Silvana Pilotti[5], and Roberta Maestro[6]

Abstract

Dermatofibrosarcoma protuberans (DFSP) is a rare and indolent cutaneous sarcoma. At times, a fibrosarcomatous transformation marked by a more aggressive clinical behavior may be present. We investigated the natural history and the molecular bases of progression from classic DFSP to the fibrosarcomatous form (FS-DFSP), looking, retrospectively, at the outcome of all patients affected by primary DFSP treated at our institution from 1993 to 2012 and analyzing the molecular profile of 5 DFSPs and 5 FS-DFSPs by an integrated genomics approach (whole transcriptome sequencing, copy number analysis, FISH, qRT-PCR, IHC). The presence of fibrosarcomatous features was identified in 20 (7.6%) patients out of 263 DFSP. All cases were treated with macroscopic complete surgery. A local relapse occurred in 4 of 23 patients who received a microscopic marginal surgery (2 classic DFSP, 2 FS-DFSP), while metastasis affected 2 patients, both FS-DFSP (10% of FS-DFSP), being the first event. DFSP evolution to FS-DFSP was paralleled by a transcriptional reprogramming. The recurrent loss of chromosome 22q appeared to contribute to this phenomenon by promoting the expression of epigenetic regulators, such as EZH2. Loss of the p16/CDKN2A/INK4A locus at 9p was also observed in two FS-DFSP metastatic cases.

Implications: FS-DFSP is a rare subgroup among DFSP, with a 10% metastatic risk, that was independent from local recurrence and that was not observed in DFSP, that were all cured by wide surgery. Chromosome 22q deletion might play a role in FS-DFSP, and p16 loss may convey a poor outcome. EZH2 dysregulation was also found and represents a druggable target.
Mol Cancer Res; 14(9); 820–9. ©2016 AACR.

Introduction

Dermatofibrosarcoma protuberans is a rare cutaneous sarcoma known for its indolent course, its tendency to recur mostly at the site of the primary tumor and its high cure-rate when it can be completely resected (1–3). The superficial location and the very low metastatic potential of classic dermatofibrosarcoma protuberans (DFSP) may justify a less aggressive surgical approach as compared with what applied to soft tissue sarcomas (STS). However, a fibrosarcomatous (FS) transformation may occur in 5% to 15% of DFSP, and fibrosarcomatous dermatofibrosarcoma protuberans (FS-DFSP) is associated to an increased risk of metastases, in the range of 10% to 15% (4, 5).

In most cases, the presence of fibrosarcomatous features can be detected in the primary tumor, but in some patients, it is identified only on the relapsed tumor (4, 5). Data on the proportion of patients who experience a fibrosarcomatous evolution from a pure DFSP are scanty.

DFSP and FS-DFSP are characterized by the reciprocal chromosome translocation t(17;22)(q22;q13.1) or, more often, supernumerary ring chromosome or markers derived from t(17;22), in which the collagen type Iα1 gene (*COL1A1*) on chromosome 17 is fused to the platelet-derived growth factor β-chain gene (*PDGFB*)

[1]Adult Mesenchymal Tumour and Rare Cancer Medical Oncology Unit, Cancer Medicine Department, Fondazione IRCCS Istituto Nazionale Tumori, Milan, Italy. [2]Centro Interdipartimentale di Ricerche sul Cancro G. Prodi, Università di Bologna, Bologna, Italy. [3]Melanoma and Sarcoma Unit, Department of Surgery, Fondazione IRCCS Istituto Nazionale Tumori, Milan, Italy. [4]Dipartimento di Medicina Sperimentale, Specialistica e Diagnostica, Università di Bologna, Bologna, Italy. [5]Department of Diagnostic Pathology and Laboratory, Laboratory of Experimental Molecular Pathology, Fondazione IRCCS Istituto Nazionale Tumori, Milan, Italy. [6]Unit of Experimental Oncology 1, CRO Aviano National Cancer Institute, Aviano, Italy. [7]Unit of Immunotherapy of Human Tumors, Fondazione IRCCS Istituto Nazionale Tumori, Milan, Italy. [8]Department of Anatomic Pathology, General Hospital of Treviso, Treviso, Italy.

Note: Supplementary data for this article are available at Molecular Cancer Research Online (http://mcr.aacrjournals.org/).

A. Astolfi, S. Pilotti, and R. Maestro contributed equally to this article.

Prior presentation: Preliminary account of this study has been presented at ASCO Annual Meeting, 2015, Chicago, IL (abstract 10554).

Corresponding Author: Silvia Stacchiotti, Fondazione IRCCS Istituto Nazionale Tumori, via Venezian 1, Milan 20133, Italy. Phone: +3902-2390-2182; Fax: +390223902804; E-mail: silvia.stacchiotti@istitutotumori.mi.it

doi: 10.1158/1541-7786.MCR-16-0068

Published OnlineFirst June 2, 2016; DOI: 10.1158/1541-7786.MCR-16-0068

on chromosome 22. The resulting upregulation of the PDGFB protein activates the PDGFB receptor (PDGFRB), inducing tumor growth through an autocrine–paracrine loop (4, 6, 7).

COL1A1–PDGFB rearrangement is of major help in confirming the diagnosis in those cases in which the classic component is completely lost (4, 8). *COL1A1–PDGFB* retainment in FS-DFSP suggests that other still undetermined genetic abnormalities account for progression of DFSP to FS-DFSP.

Therefore, we investigated the natural history of DFSP evolution to FS-DFSP in patients presenting to the Fondazione IRCCS Istituto Nazionale dei Tumori (Milan, Italy; INT) with a primary lesion, from 1993 to 2012. In addition, we molecularly profiled a set of DFSP and FS-DFSP by a combined approach, including whole transcriptome sequencing, copy number analysis, FISH, qRT-PCR, and immunohistochemical investigations, to gain insights into the molecular bases of fibrosarcomatous progression and to identify possible prognostic factors and druggable targets.

Patients and Methods

All consecutive patients affected by primary DFSP, located at any site, and treated at INT from January 1993 to December 2012 were considered, including only patients admitted for primary DFSP, either for initial treatment or reexcision after a previous inadequate surgery performed elsewhere. Patients with recurrent disease, defined as tumor regrowth at the original tumor site at least 6 months after treatment at another institution, were excluded. Data were extracted from a prospectively maintained database, including all adult patients with STS treated at INT.

In all cases, diagnosis was confirmed by an expert pathologist (S. Pilotti). All surgical excisions were macroscopically complete and classified according to the closest surgical margin, which was microscopically categorized as positive (tumor within 1 mm from the inked surface, R1) or negative (absence of tumor within 1 mm from the inked surface, R0). Before surgery, all patients underwent staging with chest X-ray or CT scan.

After surgery, all patients were followed up every 6 months for the first 5 years and then every year for, at least, 5 more years. Generally, follow-up included a clinical exam, local ultrasound or MR, along with a chest X-ray or chest CT every other visit. Last follow-up was defined as a patient's last recorded visit at INT at the time of data collection. Local recurrence (LR) and distant metastasis (DM) were confirmed with a biopsy in all cases.

Overall survival (OS) and crude incidence of LR and DM were evaluated. Events were considered the first evidence of local or distant relapse for crude cumulative incidence (CCI) of LR or CCI of DM and death related to any cause for OS. Event times were computed from the date of surgery to the date of the event occurrence.

To gain insights into mechanisms involved in fibrosarcomatous progression, tumor samples from 5 patients suffering from DFSP and 5 patients with FS-DFSP were collected for molecular profiling. Peripheral blood sample collection from each patient included in the translational study was also planned upfront in case the assessment of somatic/germline status of putative mutation(s) had to be determined. These cases were selected on the basis of the availability of frozen samples and peripheral blood and did not belong to the surgical series, having been operated on after 2012.

This retrospective study was approved by the ethics committee of INT.

Pathology, immunophenotyping, and FISH analysis

Fibrosarcomatous change was defined by the appearance in a classical storiform DFSP of at least 5% of high cellular area made up of spindle cells arranged in an herringbone pattern with a mitotic index >7/10 high power fields (9); necrosis, pleomorphic features, and myofibroblastic differentiation were also recorded and considered in making FS-DFSP diagnosis, as well as decrease/disappearance of CD34 immunoreactivity (10). Notably, in the current series, with the exception of case D6 in Table 1, which presented both components, fibrosarcomatous change accounted for more than 90%. IHC was performed using antibodies directed against the following proteins: Ki67, INI1, TWIST1, SNAI2/SLUG, ZEB1, EZH2, and p16. Detailed antibody information and staining conditions are provided in Supplementary Information S1.

FISH analyses were performed on 2-μm thick formalin-fixed paraffin-embedded (FFPE) tissue sections by using the indicated BAC probes (Children Hospital Research Institute, Oakland, CA): *PDGFB*, RP11-630N12 at the telomeric end and RP11-506F7 at centromeric end; *COL1A1*, RP11-131M15 at the telomeric end and RP11-93L18 at centromeric end.

BACs were labeled in SpectrumGreen (SG) or SpectrumOrange (SO; Abbott Molecular) by nick translation (Abbott Molecular). Probe labeling and FISH slide preparation were carried out according to standard protocols. The presence of the rearrangement was revealed by using either SG-labeled *COL1A1* BAC probes together with SO-labeled *PDGFB* probes (*COL1A1–PDGFB* fusion) or differentially labeled (centromeric in SO, telomeric in SG) *PDGFB* probes (*PDGFB* break apart).

CDKN2A/p16 gene status was assessed by FISH on 2-μm thick FFPE tissue sections using the Vysis LSI *CDKN2A/CEP 9* (Abbott Molecular).

Whole transcriptome sequencing (RNA-seq)

Detailed methodologic procedures are provided in Supplementary Information S1. Briefly, whole transcriptome sequencing (RNA-seq) was performed on RNA isolated from fresh-frozen samples of 5 DFSP and 5 FS-DFSP using the TruSeq RNA Sample Prep v2 protocol (Illumina). An average of 94.5 million reads per sample was obtained.

The short reads were mapped on the human reference genome by TopHat/Bowtie pipeline. Large chromosomal rearrangements were detected with DeFuse, ChimeraScan, and FusionMap tools. For gene expression profile, after the calculation of normalization factors to scale the raw library size (*calcNormFactors* method), the functions *lmFit* followed by *eBayes* were adopted to perform the DE computation. Unsupervised principal component analysis (PCA) was performed with TM4-MEV (http://www.tm4.org) and visualized with the R package *lattice*.

Gene enrichment and prioritization were analyzed by using ToppGene, GSEA, WebGestalt, and PGE suites.

SNP array and copy number analysis

Genomic DNA was extracted with QIAamp DNA Mini Kit (Qiagen), labeled, and hybridized to Cytoscan HD Arrays (Affymetrix) following the manufacturer's instructions. Quality was checked by SNP QC and MAPD calculation. Copy number analysis was performed with Chromosome Analysis Suite (ChAS) Software, by applying hidden Markov model algorithm to detect amplified and deleted segments, with respect to a normal reference model file. To control for hyperfragmentation, adjacent

Published OnlineFirst June 2, 2016; DOI: 10.1158/1541-7786.MCR-16-0068

segments separated by <50 probes were combined into one single segment, and only segments >50 probes were considered.

qRT-PCR analysis

Expression analysis of *EZH2*, *HOTAIR*, *H19*, *let-7a*, and *let-7b* was performed by qRT-PCR on a CFX96 Real-Time Apparatus (Bio-Rad). All experiments were performed in triplicate and repeated at least twice. Detailed methodologic procedures are provided in Supplementary Information S1.

Results

Clinical findings

A total of 263 patients were identified. A total of 243 (92.4%) patients were affected by DFSP and 20 (7.6%) by FS-DFSP. Main patient characteristics are listed in Table 2. *COL1A1–PDGFB* fusion gene was confirmed by FISH in 18 of 20 FS-DFSP cases, whereas in 2 of 20 cases, FISH analysis was not performed due to lack of material.

The two groups of patients shared similar clinical characteristics. Microscopic surgical margins were positive in 23 (8.8%), 21 of 243 (8.6%) DFSPs, and 2 of 20 (10%) FS-DFSPs, respectively. Among patients with positive surgical margins, 13 cases (56.5%) had the tumor located in the head and neck, 5 in the trunk (2 of them at sternoclavicular area, partially involving the neck), 5 in the extremities (1 involved the foot and 2 the groin/urogenital area).

Patient outcome. Median follow-up from the time of definitive surgery was 85 (range 12–194) months. At the time of the current analysis, 261 of 263 patients are alive and 2 of 263 are dead from other diseases. None of the patients is dead of disease and 2 patients are alive with metastatic disease.

Overall, 5/10/15–year OS were 99%/99%/93%, respectively.

LR occurred in 4 patients (1.5%), being in all the first event, following an R1 resection of the primary tumor in all 4 cases. Local relapse occurred in 2 of 21 (9.5%) DFSPs and in 2 of 2 (100%) FS-DFSPs operated on with positive microscopic margins. None of these patients subsequently developed DM. The other 18 patients operated on with positive margins remained disease free at a median follow-up of 96 months after surgery (range 19–147).

Two patients affected by FS-DFSP developed DM (0.76% of the whole series; 10% of FS-DFSP), whereas none of the patients affected by DFSP ever developed metastatic disease. The 5-, 10-, 15-year incidence of DM was 0%/0%/0% and 5%/10%/10% in DFSP and FS-DFSP, respectively. In all cases, DM was the first event. Metastases were located to the lung (1) and the pancreas (1). DM occurred after 26 and 125 months. The presence of the fusion gene (*COL1A1–PDGFB*) in the metastatic tissue was confirmed in all cases.

Molecular profiling of DFSP evolution

Tumors and peripheral blood from 10 patients suffering from DFSP (5) and FS-DFSP (5), operated on at INT after 2012, were collected. The characteristics of the tissue samples molecularly evaluated are summarized in Table 1 and in Supplementary Table S1. In particular, they were all derived from different patients (no pair-matched samples are included), from the primary tumor in 6 cases, local relapse in 2, and distant metastasis in 2. All cases but one were histologically homogeneous throughout the tumor sample; one case (D6, Table 1) exhibited instead both classic and fibrosarcomatous components (Fig. 1). At frozen section control, performed in all the cases, sampling of this case felt in the DFSP area.

FISH confirmed the presence of *COL1A1–PDGFB* in all cases. High levels of *COL1A1–PDGFB* fusion copy number/amplification was observed in 3 cases: 2 FS-DFSPs (D2, D4) and one DFSP (D6). No strong evidence of intratumoral heterogeneity for the fusion was observed, with the exception of the cases showing *COL1A1–PDGFB* amplification.

Whole transcriptome sequencing reveals a role for extracellular matrix remodeling and EMT in fibrosarcomatous evolution. The gene expression profile was computed from whole transcriptome data and compared between the 5 DFSP and 5 FS-DFSP tumors. Unsupervised PCA of gene expression data showed that the DFSP group had a transcriptome profile highly homogenous. A considerable degree of heterogeneity was instead observed among FS-DFSP, with one case (D3/L168) clustering with DFSP (Supplementary Fig. S1). Gene expression analysis identified 439 differentially expressed transcripts, with 174 upregulated and 265 downregulated genes in FS-DFSP compared with DFSP (log2 fold change greater than +0.6; Supplementary Table S2).

Pathway analysis (Supplementary Table S2) highlighted an enrichment in GO-biological process terms related to extracellular matrix (ECM) organization, extracellular structure organization, cell migration, collagen fibril organization, locomotion, and collagen metabolic process, beside morphogenesis, neuro- and vasculogenesis, and cell proliferation. These analyses also pinpointed to a role for ECM and ECM–receptor interaction. Highly overrepresented Reactome terms included ECM organization and collagen formation, and ECM–receptor interaction was the top list term in KEGG pathways. Pathway analysis failed to underscore a significant involvement of an adaptive immune response in fibrosarcomatous evolution.

Twenty-nine genes differentially expressed in FS-DFSP versus DFSP belonged to the "epithelial–mesenchymal transition (EMT) hallmark gene signature," according to the GSEA Hallmark gene sets ($P = 6.97E{-}24$). Moreover, our dataset overlapped with the DNA methylation map of pluripotent and differentiated cells (66 genes; ref. 11) and with GSEA C2 curated datasets related to stemness (Supplementary Table S2). On these grounds, we investigated by IHC the expression of three major EMT regulators, that is, *TWIST1*, *SNAI2/SLUG*, and *ZEB1*. Besides acting as EMT regulators, these transcription factors are also involved in stem cell maintenance, mesoderm development, and neural crest specification. Intriguingly, FS-DFSP displayed an increased number of decorated nuclei for any of the three EMT master regulators tested (Supplementary Fig. S5). These genes did not emerge as differentially expressed by transcriptome sequencing analysis, but their protein product is known to undergo posttranscriptional regulation (12, 13).

Molecular data integration suggests a role for 22q loss in fibrosarcomatous evolution. Positional gene enrichment analysis unveiled that a significant fraction of genes modulated during the transition from DFSP to FS-DFSP belonged to the 22q13 and 12q chromosome regions (Supplementary Table S2). In particular, of the 24 genes significantly modulated mapping on 22q, 16 were downregulated in FS-DFSP. These downregulated genes were all telomeric to *PDGFB*, whereas those centromeric to *PDGFB* tended to be upregulated.

Published OnlineFirst June 2, 2016; DOI: 10.1158/1541-7786.MCR-16-0068

Table 1. Characteristics of the tissue samples molecularly profiled

Sample ID	Origin of the tissue sample molecularly profiled	Path diagnosis	FISH analysis *COL1A1/PDGFRB*	Primary tumor site	Prior medical treatment
D1	Primary tumor	DFSP	Positive	Skin	Naïve
D2	Metastasis (retroperitoneum)	FS-DFSP	Positive	Skin	Chemotherapy and radiotherapy
D3	Primary tumor	FS-DFSP	Positive	Skin	Naïve
D4	Primary tumor	FS-DFSP	Positive	Skin	Naïve
D5	Local relapse	FS-DFSP	Positive	Skin	Naïve
D6	Primary tumor	DFSP	Positive	Skin	Naïve
D7	Primary tumor	DFSP	Positive	Skin	Naïve
D8	Primary tumor	DFSP	Positive	Skin	Naïve
D9	Metastasis (lung)	FS-DFSP	Positive	Scalp	Naïve
D11	Primary tumor	DFSP	Positive	Skin	Naïve

To get insights on these findings, 5 DFSPs and 5 FS-DFSPs were analyzed by SNP array to identify copy number variations (CNV). CNV data were then integrated with the fusion transcript detection performed on RNA-seq data to build the complete picture of genomic structural variations (Fig. 2; Supplementary Table S3). Several alterations were estimated as mosaic and thus were representative of the clonal architecture of the tumor.

DFSPs were characterized by several macroscopic and few focal amplifications or deletions (mean: 7.7 regions for sample). On the contrary, FS-DFSP carried numerous alterations with a relevant increase of focal amplifications and deletions (mean: 27.2 regions for sample). Interestingly, the only fibrosarcomatous patient carrying a lower number of genomic alterations (D3) was the one showing a gene expression profile clustering with DFSP. Among the 182 altered genomic regions, the majority (69%) were gains of one or more copies. DFSP and FS-DFSP shared gains of 3 or more copies of the chromosomal regions flanking the *COL1A1–PDGFB* breakpoint. Namely, gain of the entire 17q21.33-q25.3 of chromosome 17 region (telomeric to *COL1A1*) and gain of the 22q12.3-q13.1 region (centromeric to *PDGFB*) were detected in all cases. FS-DFSP tended to show a higher frequency of copy number losses compared with DFSP. Gain of the whole chromosome 12 was observed in 2 of 5 FS-DSFPs, a finding that is in line with RNA-seq cytoband gene enrichment analysis. Macroscopic amplification of chromosome 5 was detected in 3 FS-DFSPs and 2 DFSPs, these latter carrying also gain of chromosome 1 and 4. One DFSP carried an extra copy of chromosome 8. Gains of chromosome 4, 5, 8, and 12 have been previously reported in DSFP (14).

Interestingly, in line with *in silico* predictions based on RNA-seq data, SNP array analysis highlighted the deletion of the 22q13-ter chromosome region, just telomeric to the PDGFB breakpoint, in 4 FS-DFSP. Loss of 22q13-ter was observed also in the classic component of the tumor (case D6) that displayed both components and was the only locally relapsed DFSP included in the study (Fig. 3A).

Apart from few discrepancies (likely due to intratumoral heterogeneity, nontumoral cell contamination, complex, and cryptic rearrangements), FISH analyses supported SNP array data and corroborated the involvement of chromosome 22 loss in fibrosarcomatous evolution. Precisely, beside the translocated alleles (one in case D5, 2–3 in cases D1, D3, D7, D8, D9, D11, and more than three in cases D2, D4, D6) and two intact *COL1A1* genes, all but one DFSP carried two nontranslocated *PDGFB* alleles (chromosome 22), whereas all FS-DFSP retained just one copy (Fig. 3B and C and Supplementary Fig. S3). The patterns observed fit well with the features of the DFSP t(17;22) rearrangement as described in classic cytogenetics (see Cancer Genome Anatomy Project, http://cgap.nci.nih.gov/), which, with the exception of the juvenile forms (not included in this study), is typically unbalanced in origin. Indeed, the most frequent abnormality reported is the presence of one or more copies of a der(22) t(17;22) or related rings/marker chromosomes, together with two copies of normal chromosome 17. Moreover, in the majority of DFSP karyotypes, two copies of a normal chromosome 22 are also present, while the remaining karyotypes (about 1/3 in the Cancer Genome Anatomy Project files) show a single intact copy of chromosome 22. Intriguingly, in our series, the presence of one single copy of nontranslocated PDGFB/nontranslocated chromosome 22 segregated with the fibrosarcomatous form. Taken together, our results indicate that the detection of chromosome 22q13-ter loss by SNP array likely reflects the retention of a single intact chromosome 22 in FS-DFSP.

A scrutiny of the potential tumor suppressor genes mapping within the 22q13-ter deleted region in FS-DFSP pointed to the

Table 2. Main patient characteristics

	Classic DFSP *N* (%)	FS-DFSP *N* (%)	Total *N* (%)
Patients	243 (92.4)	20 (7.6)	263 (100)
Gender			
Female	116 (47.7)	7 (35)	123 (46.7)
Male	127 (52.3)	13 (65)	140 (53.3)
Patient's age, years			
Median (range)	39 (18–80)	40 (26–80)	39 (18–80)
Tumor size, cm			
Median (range)	2 (1–20)	6 (1–11)	2 (1–20)
Surgical margins			
R0	222 (91.4)	18 (90)	240 (91.2)
R1	21 (8.6)	2 (10)	23 (8.8)
Site			
Extremities	148 (61)	14 (70)	162 (61.6)
Trunk	69 (28.3)	4 (20)	73 (27.7)
Head & Neck	26 (10.7)	2 (10)	28 (10.7)
Preoperative imatinib			
Done	4 (1.6)	1 (5)	5 (1.9)
Not done	239 (98.4)	19 (95)	258 (98.1)
Postoperative RT			
Done	4 (1.6)	1 (5)	5 (1.9)
Not done	239 (98.4)	19 (95)	258 (98.1)

Abbreviation: RT, radiotherapy.

Published OnlineFirst June 2, 2016; DOI: 10.1158/1541-7786.MCR-16-0068

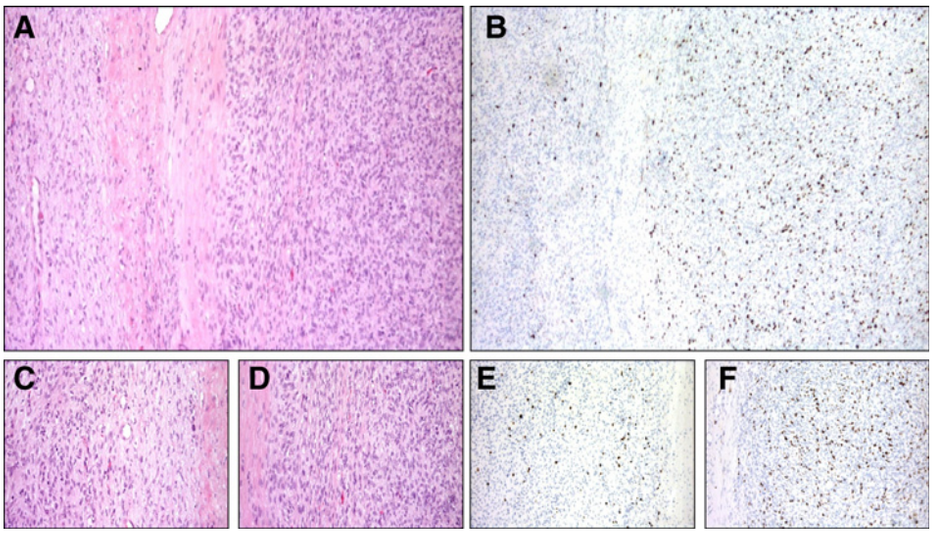

Figure 1.
Case D6. **A,** hematoxylin and eosin (H/E) staining [DFSP (left) with fibrosarcomatous overgrowth (right)]. **B,** a serial section immunolabeled with Ki67 antibody. **C–F,** higher magnification of the corresponding low- and high-grade proliferation areas of **A** and **B,** respectively.

presence of two members of the let-7 family of miRNA, *let-7a-3* and *let-7b*. qRT-PCR confirmed the downregulation of *let-7a* and *let-7b* in 22q deleted FS-DFSP (Fig. 3D). Intriguingly, these miRNAs have been shown to target, among the others, EZH2 (see below).

Both SNP array and FISH analyses pinpointed a possible role of 9p21 loss in metastatic evolution of FS-DFSP. In fact, SNP array revealed high instability of the 9p chromosome region, with multiple deletions of one copy and homozygous loss of the 9p21.3 cytoband, in the 2 FS-DFSP metastatic cases (D2, D9). This chromosome region harbors the *p16/INK4A/CDKN2A* locus. The deletion of *CDKN2A* was confirmed by FISH and correlated with loss of p16 expression, as detected by IHC (data not shown).

Finally, integration of SNP array and RNA-seq data indicated that, beside the pathognomonic *COL1A1–PDGFB* chimera, FS-DFSP expressed several additional fusion genes (Supplementary Table S3), indicating a high degree of genomic instability.

EZH2 is a candidate target in DFSP The overlap of the transcriptional profile of FS-DFSP with the DNA methylation map of pluripotent and differentiated cells (Supplementary Table S2; ref. 11) suggested a role for epigenetic remodeling in fibrosarcomatous evolution. Immunohistochemical analyses ruled out a role for INI1 loss in FS-DFSP pathogenesis (data not shown). Instead, the integration of molecular analyses suggested a role for the H3K27 methyltransferases EZH2, a component of the polycomb repressive complex 2. In fact, *H19* and *HOTAIR*, two noncoding RNAs involved in the regulation of the activity of EZH2, were among the genes most significantly upregulated in FS-DFSP. The elevated expression of these long noncoding RNAs in FS-DFSP was confirmed by qRT-PCR (Supplementary Fig. S4). Although *EZH2* was not included in the set of genes detected as differentially expressed by RNA-seq, immunohistochemical analyses revealed an increased number of EZH2 immunolabeled nuclei in FS-DFSP with respect to DFSP cases, which was paralleled by a higher Ki67 score (Fig. 4 and Supplementary Fig. S5). qRT-PCR confirmed higher expression levels of *EZH2* among FS-DFSP (Supplementary Fig. S4). Intriguingly, EZH2 is among the targets of two miRNAs, *let-7a* and *let-7b*, that map in the 22q region that was found deleted in FS-DFSP.

Discussion

In this retrospective series, fibrosarcomatous transformation was confirmed to be a rare event that affected only 20 (7.6%) of 263 patients surgically treated for a primary DFSP. All FS-DFSP carried the *COL1A1–PDGFB* fusion gene. In DFSP, negative margin resection was always curative. No DFSP patient suffered from distant relapses. Local relapses were observed only in patients treated with R1 resection. Metastases occurred only in 2 patients with FS-DFSP (0.76% of the whole series; 10% of FS-DFSP), and it was the first event. The molecular profiling of a subset of 10 cases (5 DFSP and 5 FS-DFSP) indicated that the fibrosarcomatous progression is sustained by a transcriptional reprogramming, which is paralleled by loss of genomic material from a nontranslocated chromosome 22q. In addition, loss of the short arm of chromosome 9, including the *p16/CDKN2A/INK4A* locus, was detected in the 2 metastatic FS-DFSP samples. EZH2 emerged as a promising druggable target.

We found fibrosarcomatous changes in a minority of cases (7.6%), with available series being consistent with a 5% to 20% rate of fibrosarcomatous transformation (1–4). Of course, institutional referral biases as well as sampling issues especially in oldest cases may be relevant. No differences were detected in sex, age, and anatomic location between DFSP and FS-DFSP. As we had already described (2), in this more recent and larger series, focused only on primary cases, we confirm that negative margin resection was always curative for DFSP and prevented LR (not DM) in FS-DFSP as well. The only factor associated to a metastatic risk was the presence of fibrosarcomatous features. However, this risk was low, and the majority of patients with a fibrosarcomatous transformation were also cured by surgery alone. By contrast, none of DFSP patients developed metastasis. Interestingly, none of our FS-DFSP patients with DM had an LR, suggesting that DM may be inherently related to tumor biology. By contrast, quality of surgical margin was not related to the histology but to the presence of a critical anatomic location. In

Published OnlineFirst June 2, 2016; DOI: 10.1158/1541-7786.MCR-16-0068

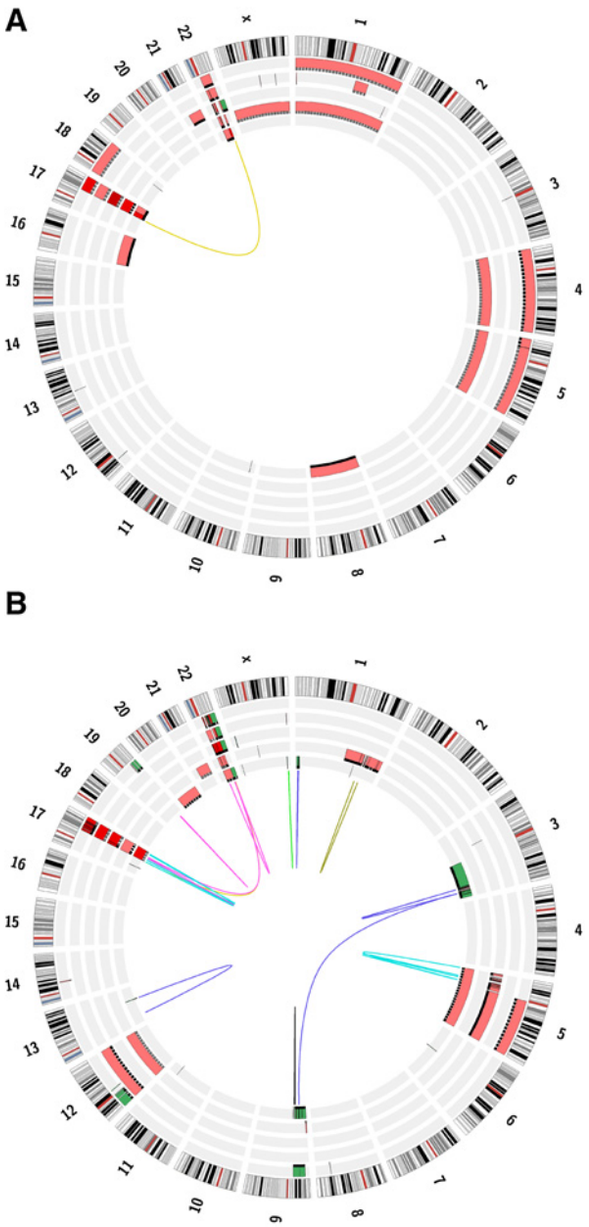

Figure 2.

Circo plots representing genomic structural variants carried by DFSP (**A**) and FS-DFSP (**B**). The graph shows the chromosomes arranged in a circular orientation. Rings identify the patients, colored tracks regions of copy number alteration. Color code: dark green, homozygous deletion; light green, heterozygous deletion; light red, gain of one copy; dark red, copy number >3; grey dotted line, <50% mosaic alteration; black dotted line, >50% mosaic alteration; black line, full copy number gain or loss. Colored lines connect positions that participate in genomic rearrangements giving rise to fusion transcripts.

particular, the LR risk was nil also for FS-DFSP patients, when margins were negative. This supports the notion that a wide surgical resection still remains the gold standard in both DFSP and FS-DFSP.

Cases of fibrosarcomatous transformation occurring over time in DFSP after multiple local relapses are described in other reports (8). We cannot challenge this possibility, as the proportion of patients who relapsed was very low. On the other side, a wide resection or a reexcision in case of positive margins should always be considered in FS-DFSP, given the risk of developing metastatic disease (2, 4, 8), while positive surgical margins may still be accepted in DFSP, especially when cosmesis is an issue. It is therefore evident the importance of an adequate tumor sampling and of correct pathologic diagnosis in decision making.

We ran a set of molecular investigations aimed at shedding light on the mechanisms of fibrosarcomatous evolution and, ideally, at identifying markers of prognostic and predictive value. To this end, we initially compared the transcriptome profile of 5 DFSPs and of 5 FS-DFSPs. All samples expressed the *COL1A1–PDGFB* fusion transcript, with no significant variation in its expression levels between DFSP and FS-DFSP, as previously reported (4, 8). No other recurrent fusion transcripts that may hallmark the FS-DFSP variant were detected.

Pathway analysis ruled out a major role for the immune response in fibrosarcomatous evolution of DFSP and suggested instead an involvement of tumor microenvironment and ECM remodeling. In particular, the switch from DFSP to FS-DFSP was paralleled by an enrichment in genes belonging to the EMT gene signature, as defined by Gröger and colleagues (15). The EMT program has been linked to aggressive tumor behavior, and modulation of mesenchymal traits toward a more undifferentiated state has been previously reported to play a pivotal role in sarcoma development and progression (16–21). EMT is governed by a set of transcription factors, including TWIST1, SNAI2/SLUG, and ZEB1. Here, we demonstrate that these proteins are markedly increased in FS-DFSP compared with DFSP. Noteworthy, the EMT program involves epigenetic remodeling with DNA and histone modifications (21).

Our study suggests that DFSP evolution to FS-DFSP might be correlated to loss of chromosome material involving the 22q region telomeric to PDGFB. In fact, a significant fraction of genes detected by RNA-seq as modulated in FS-DFSP compared with DFSP turned out to belong to the long arm of chromosome 22, which bears the *PDGFB* gene. In particular, FS-DFSP exhibited downregulation of genes telomeric to *PDGFB* (22q13-ter). This was is in keeping with SNP array data, which highlighted in FS-DFSP recurrent loss of material from the 22q-ter chromosome region. FISH analyses indicated that the pattern observed was compatible with the loss of one copy of nontranslocated chromosome 22. To the best of our knowledge, 22q loss, although occasionally reported (22–28), has never been associated to fibrosarcomatous evolution.

Previously, fibrosarcomatous transformation of DFSP had been correlated to the amplification of *COL1A1–PDGFB* fusion, an association that we and others failed to confirm (4, 22). Also in the series here analyzed, both DFSP and FS-DFSP shared extra copies of the chromosome material flanking the *COL1A1–PDGFB* breakpoint, ruling out a major role for *COL1A1–PDGFB* amplification in fibrosarcomatous evolution.

Chromosome 22q loss, in form of deletion or monosomy, is a recurrent event in different types of cancer, comprising GIST and rhabdoid tumors (29–32), and several minimal deleted regions, including 22q13-ter (33), have been identified harboring putative tumor suppressor genes. Interestingly, a scrutiny of the genes targeted by the 22q13-ter loss in FS-DFSP

Published OnlineFirst June 2, 2016; DOI: 10.1158/1541-7786.MCR-16-0068

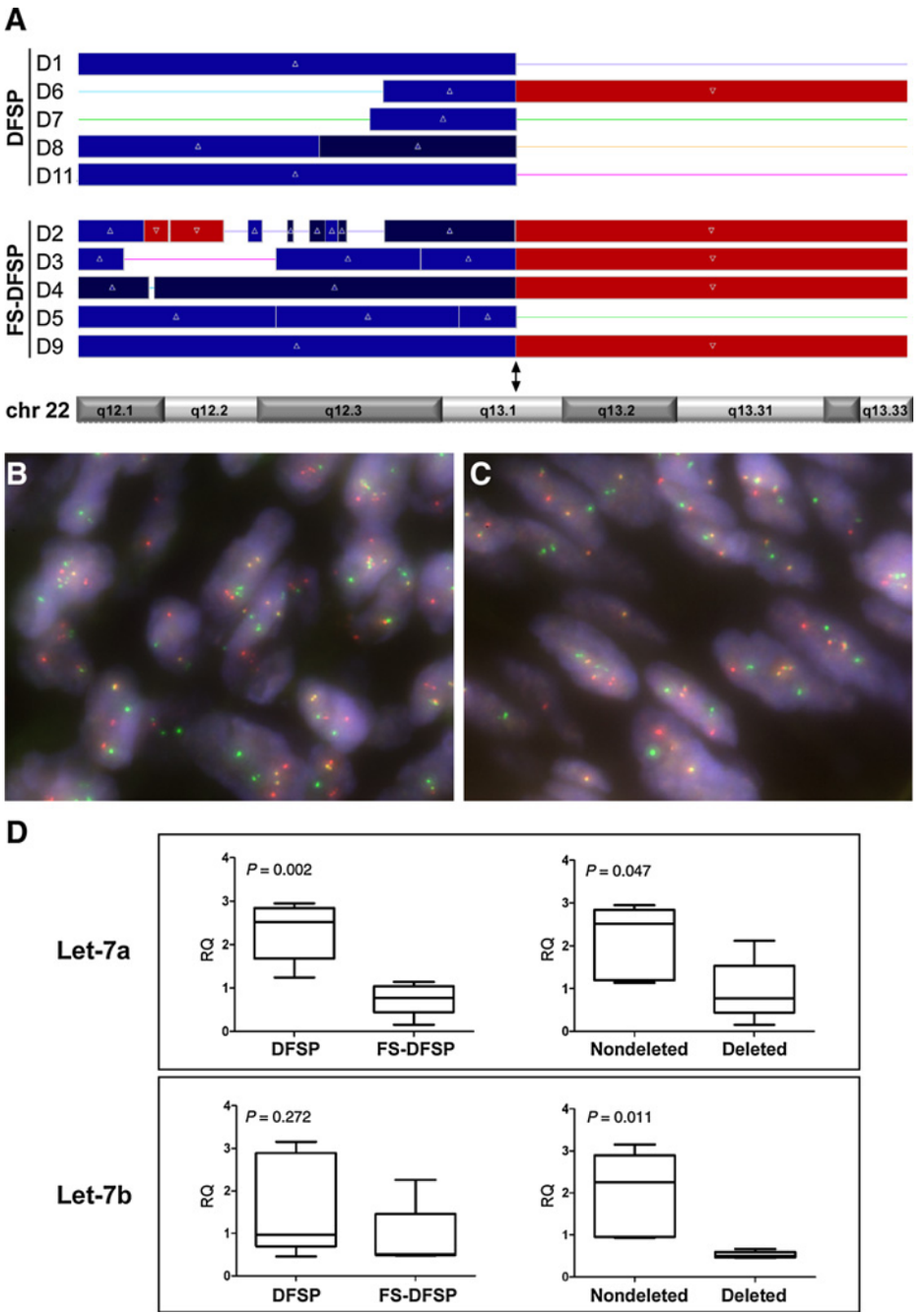

Figure 3.
Chromosome 22q13-ter loss in FS-DFSP. **A,** graphical representation of copy number (CN) gains and losses on chromosome 22q in DFSP (cases D1, D6, D7, D8, D11) and FS-DFSP (cases D2, D3, D4, D5, D9). Colored lines, CN = 2 (diploid region); red bar, CN = 1; blue bar, CN = 3; deep blue bar, CN > 3. Arrow, PDGFB breakpoint at 22q13.1. **B** and **C,** COL1A1 (SG) and PDGFB (SO) probes. Two fusion signals, together with 2 free red and 2 free green signals corresponding to intact copies of PDGFB and COL1A1, respectively, were detected in DFSP cells (case D8 is shown as an example; **B**). The presence of 2 fusion signals, 2 green signals, and one single free red signal in FS-DFSP cells supports the loss of chromosome 22q in fibrosarcomatous evolution (case D9; **C**). These patterns were coherent with PDGFB break apart FISH (Supplementary Fig. S5). **D,** Let-7a and Let-7b gene expression in DFSP and FS-DFSP. Plots show the relative quantification (RQ) by qRT-PCR of let-7a and let-7b expression in DFSP versus FS-DFSP and in 22q13-ter deleted versus nondeleted samples. Statistical *P* values (unpaired Student *t* test) are indicated.

pointed to 2 members of the *let-7* family of miRNAs, *let-7a* and *let-7b*. *Let-7* genes encode tumor suppressor miRNAs that control the expression of a number of proteins involved in proliferation and apoptosis, EMT, adhesion, and migration (34, 35). Among others, *let-7* miRNAs have been implicated in the regulation of components of the epigenetic machinery, namely EZH2 (36). EZH2 is the catalytic subunit of the polycomb repressive complex 2 (PRC2) that typically controls histone methylation–mediated gene repression via local chromatin reorganization, but it may also act as a gene activator through a PRC2-independent route. EZH2 plays a critical role in cancer development and progression by epigenetically altering the gene expression program (37, 38). Molecular analyses confirmed the downregulation of *let-7a* and *let-7b* in FS-DFSP, and IHC showed an increase of EZH2-immunolabeled nuclei in FS-DFSP. Moreover, 2 noncoding RNAs involved in the regulation of EZH2, *H19*, and *HOTAIR* (39–41) turned out to be among the RNAs most significantly upregulated in FS-DFSP. This finding suggests that overexpression of *H19* and *HOTAIR*, together with *let-7* downregulation, all concur to induce EZH2 and, in turn, chromatin remodeling and mesenchymal transdifferentiation in FS-DFSP (19, 39–41).

Published OnlineFirst June 2, 2016; DOI: 10.1158/1541-7786.MCR-16-0068

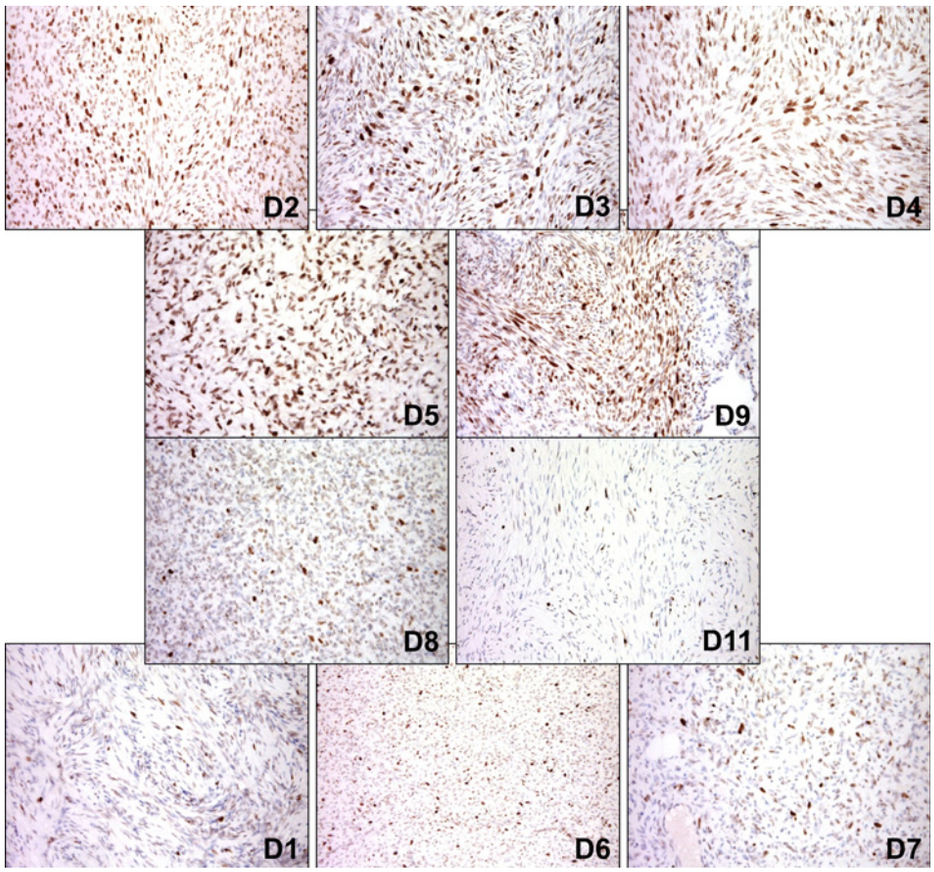

Figure 4.
EZH2 staining. Imaging gallery demonstrating the marked increase of EZH2-decorated nuclei in FS-DFSP (top row) when compared with DFSP (bottom row).

A role for epigenetic reprogramming in fibrosarcomatous transformation was also supported by the finding that 66 genes enriched in FS-DFSP versus DFSP are reported to undergo epigenetic regulation (11), and recent evidence is consistent with the involvement of chromatin remodeling in translocation-associated sarcomas (42). Overall, our analyses point at EZH2 as a promising target in DFSP. Remarkably, selective inhibitors of EZH2 are now available in the clinic. In particular, the EZH2 inhibitor tazemetostat is entering a phase III clinical study in *INI1* deleted sarcoma by virtue of a functionally antagonistic relationship between PcG proteins and SWI/SNF complex (43). Our study suggests that this class of drug could be interesting in advanced FS-DFSP, even though EZH2 upregulation is mediated here by mechanism other than the deletion of *INI1/SMARCB1*.

Structural variation analysis revealed a loss of the short arm of chromosome 9 (9p21), that harbors the *CDKN2A locus*, in the two metastatic samples included in the study. Interestingly, none of the other patients of the current series has developed metastasis to date. The *CDKN2A* locus encodes *p16/INK4A*, an inhibitor of cyclin D–CDK4/6 complexes, and *p14ARF* that negatively controls HDM2-mediated ubiquitination and degradation of p53. Loss of the *CDKN2A* promotes uncontrolled cell proliferation and tumor progression (44). In our series, *CDKN2A* homozygous deletion correlated with loss of p16 expression, as indicated by FISH and IHC. Our finding, which is in line with a recent report by Eilers and colleagues (45), indicates that p16 loss might identify a subset of DFSP/FS-DFSP with poor prognosis. Noteworthy, an epigenetic link between p16 loss and EZH2 expression has been recently suggested (46). The evaluation of p16 gene copy number in the primary tumor of FS-DFSP patients included in the surgical series is ongoing to investigate to what extent this alteration is present at disease onset and correlates with the development of distant metastasis.

Overall, our study confirms that fibrosarcomatous evolution is a rare event in DFSP, marked by a low metastatic risk. Interestingly, none of DFSP patients suffered from distant relapse, and all cases were cured by negative margin surgery. This should be used to inform treatment decision for both DFSP variants. The molecular profiling of DFSP and FS-DFSP implicated EMT and epigenetic remodeling and unveiled a possible role for chromosome 22q13-ter loss in fibrosarcomatous evolution and *CDKN2A/p16* loss in dismal prognosis, findings that are worthy of further investigation in larger series. The finding that EZH2 is upregulated in FS-DFSP discloses novel therapeutic opportunities for this subset of tumors.

Disclosure of Potential Conflicts of Interest

S. Stacchiotti reports receiving a commercial research grant from Novartis. A. Gronchi has received speakers bureau honoraria from and is a consultant/advisory board for Novartis. M.A. Pantaleo reports receiving a commercial research grant from Novartis. P.G. Casali has received speakers bureau honoraria from and is a consultant/advisory board for Novartis. No potential conflicts of interest were disclosed by the other authors.

Published OnlineFirst June 2, 2016; DOI: 10.1158/1541-7786.MCR-16-0068

Authors' Contributions

Conception and design: S. Stacchiotti, A. Astolfi, A. Gronchi, M.A. Pantaleo, A.P. Dei Tos, C. Castelli, G.P. Dagrada, S. Pilotti, R. Maestro
Development of methodology: S. Stacchiotti, M. Urbini, A.P. Dei Tos, G.P. Dagrada
Acquisition of data (provided animals, acquired and managed patients, provided facilities, etc.): S. Stacchiotti, A. Astolfi, A. Gronchi, M.A. Pantaleo, M. Brenca, M. Urbini, C. Colombo, S. Brich, P.G. Casali, G.P. Dagrada, R. Maestro, A. Fontana
Analysis and interpretation of data (e.g., statistical analysis, biostatistics, computational analysis): S. Stacchiotti, A. Astolfi, A. Gronchi, T. Negri, M. Urbini, V. Indio, S. Radaelli, A.P. Dei Tos, C. Castelli, G.P. Dagrada, S. Pilotti, R. Maestro, A. Fontana, M. Tazzari
Writing, review, and/or revision of the manuscript: S. Stacchiotti, A. Astolfi, A. Gronchi, M.A. Pantaleo, T. Negri, M. Brenca, S. Radaelli, S. Brich, A.P. Dei Tos, P.G. Casali, C. Castelli, G.P. Dagrada, S. Pilotti, R. Maestro, A. Fontana, M. Tazzari
Administrative, technical, or material support (i.e., reporting or organizing data, constructing databases): S. Stacchiotti, A. Fontana
Study supervision: S. Stacchiotti, A. Gronchi

Grant Support

This work was supported by the Italian Association for Cancer Research (AIRC) and by the Italian Ministry of Health (Ricerca Finalizzata). M. Brenca is the recipient of an FIRC fellowship.

The costs of publication of this article were defrayed in part by the payment of page charges. This article must therefore be hereby marked *advertisement* in accordance with 18 U.S.C. Section 1734 solely to indicate this fact.

Received February 26, 2016; revised May 11, 2016; accepted May 16, 2016; published OnlineFirst June 2, 2016.

References

1. Fletcher CDM, Unni KK, Mertens F. World Health Organization (WHO) classification of tumours. Pathology and genetics of tumours of soft tissue and bone. Lyon, France: IARC Press; 2013. p. 80–2. Available from: https://www.iarc.fr/en/publications/pdfs-online/pat-gen/bb5/BB5.pdf.
2. Fiore M, Miceli R, Mussi C, Lo Vullo S, Mariani L, Lozza L, et al. Dermatofibrosarcoma protuberans treated at a single institution: a surgical disease with a high cure rate. J Clin Oncol 2005;23:7669–75.
3. Bowne WB, Antonescu CR, Leung DH, Katz SC, Hawkins WG, Woodruff JM, et al. Dermatofibrosarcoma protuberans: a clinicopathologic analysis of patients treated and followed at a single institution. Cancer 2000; 88:2711–20.
4. Stacchiotti S, Pedeutour F, Negri T, Conca E, Marrari A, Palassini E, et al. Dermatofibrosarcoma protuberans-derived fibrosarcoma: clinical history, biological profile and sensitivity to imatinib. Int J Cancer 2011;129:1761–72.
5. Abbott JJ, Oliveira AM, Nascimento A. The prognostic significante of fibrosarcomatous transformation in dermatofibrosarcoma protuberans. Am J Surg Pathol 2006;30:436–43.
6. Simon MP, Pedeutour F, Sirvent N, Grosgeorge J, Minoletti F, Coindre JM, , et al. et al: Deregulation of the platelet-derived growth factor B-chain gene via fusion with collagen gene COL1A1 in dermatofibrosarcoma protuberans and giant-cell fibroblastoma. Nat Genet 1997; 15:95–8.
7. Greco A, Fusetti L, Villa R, Sozzi G, Minoletti F, Mauri P, et al. Transforming activity of the chimeric sequence formed by the fusion of collagen gene COL1A1 and the platelet derived growth factor b-chain gene in dermatofibrosarcoma protuberans. Oncogene 1998; 17:1313–9.
8. Stacchiotti S, Pantaleo MA, Negri T, Astolfi A, Tazzari M, Dagrada GP, et al. Efficacy and biological activity of imatinib in metastatic dermatofibrosarcoma protuberans (DFSP). Clin Cancer Res 2016;22:837–46.
9. Goldblum JR, Folpe AL, Weiss SW. Fibrohistiocytic tumors of intermediate malignancy. In: Enzinger and Weiss's soft tissue tumors. 6th ed. Philadelphia, US: Elsevier; 2014. p. 387–400.
10. Hornick JL. Practical soft tissue pathology: a diagnostic approach. Philadelphia, Elsevier Saunders; 2013. p. 399–403.
11. Meissner A, Mikkelsen TS, Gu H, Wernig M, Hanna J, Sivachenko A, et al. Genome-scale DNA methylation maps of pluripotent and differentiated cells. Nature 2008;454:766–70.
12. Demontis S, Rigo C, Piccinin S, Mizzau M, Sonego M, Fabris M, et al. Twist is substrate for caspase cleavage and proteasome-mediated degradation. Cell Death Differ 2006;13:335–45.
13. Inoue Y, Itoh Y, Sato K, Kawasaki F, Sumita C, Tanaka T, et al. Regulation of epithelial-mesenchymal transition by E3 ubiquitin ligases and deubiquitinase in cancer. Curr Cancer Drug Targets 2016;16:110–8
14. Sirvent N, Maire G, Pedeutour F. Genetics of dermatofibrosarcoma protuberans family of tumors: from ring chromosomes to tyrosine kinase inhibitor treatment. Genes Chromosomes Cancer 2003;37:1–19.
15. Gröger CJ, Grubinger M, Waldhör T, Vierlinger K, Mikulits W. Meta-analysis of gene expression signatures defining the epithelial to mesenchymal transition during cancer progression. PLoS One 2012;7:e51136.
16. Maestro R, Dei Tos AP, Hamamori Y, Krasnokutsky S, Sartorelli V, Kedes L, et al. Twist is a potential oncogene that inhibits apoptosis. Genes Dev 1999;13:2207–17.
17. Piccinin S, Tonin E, Sessa S, Demontis S, Rossi S, Pecciarini L, et al. A "twist box" code of p53 inactivation: twist box: p53 interaction promotes p53 degradation. Cancer Cell 2012;22:404–15.
18. Alba-Castellón L, Batlle R, Francí C, Fernández-Aceñero MJ, Mazzolini R, Peña R, et al. Snail1 expression is required for sarcomagenesis. Neoplasia 2014;16:413–21.
19. Yang J, Eddy JA, Pan Y, Hategan A, Tabus I, Wang Y, et al. Integrated proteomics and genomics analysis reveals a novel mesenchymal to epithelial reverting transition in leiomyosarcoma through regulation of slug. Mol Cell Proteomics 2010;9:2405–13.
20. Tam WL, Weinberg RA. The epigenetics of epithelial-mesenchymal plasticity in cancer. Nat Med 2013;19:1438–49.
21. Malouf GG, Taube JH, Lu Y, Roysarkar T, Panjarian S, Estecio MR, et al. Architecture of epigenetic reprogramming following Twist1-mediated epithelial-mesenchymal transition. Genome Biol 2013;14: R144.
22. Salgado R, Llombart B, M Pujol R, Fernández-Serra A, Sanmartín O, Toll A, et al. Molecular diagnosis of dermatofibrosarcoma protuberans: a comparison between reverse transcriptase-polymerase chain reaction and fluorescence in situ hybridization methodologies. Genes Chromosomes Cancer 2011;50:510–7.
23. Pedeutour F, Simon MP, Minoletti F, Sozzi G, Pierotti MA, Hecht F, et al. Ring 22 chromosomes in dermatofibrosarcoma protuberans are low-level amplifiers of chromosome 17 and 22 sequences. Cancer Res 1995;55: 2400–3.
24. Pedeutour F, Simon MP, Minoletti F, Barcelo G, Terrier-Lacombe MJ, Combemale P, et al. Translocation, t(17;22)(q22;q13), in dermatofibrosarcoma protuberans: a new tumor-associated chromosome rearrangement. Cytogenet Cell Genet 1996;72:171–4.
25. Nishio J, Iwasaki H, Ishiguro M, Ohjimi Y, Yo S, Isayama T, et al. Supernumerary ring chromosome in a Bednar tumor (pigmented dermatofibrosarcoma protuberans) is composed of interspersed sequences from chromosomes 17 and 22: a fluorescence *in situ* hybridization and comparative genomic hybridization analysis. Genes Chromosomes Cancer 2001;30:305–9.
26. Buckley PG, Mantripragada KK, Benetkiewicz M, Tapia-Páez I, Diaz De Ståhl T, Rosenquist M, et al. A full-coverage, high-resolution human chromosome 22 genomic microarray for clinical and research applications. Hum Mol Genet 2002;11:3221–9.
27. Kaur S, Vauhkonen H, Böhling T, Mertens F, Mandahl N, Knuutila S. Gene copy number changes in dermatofibrosarcoma protuberans - a fine-resolution study using array comparative genomic hybridization. Cytogenet Genome Res 2006;115:283–8.
28. Linn SC, West RB, Pollack JR, Zhu S, Hernandez-Boussard T, Nielsen TO, et al. Gene expression patterns and gene copy number changes in dermatofibrosarcoma protuberans. Am J Pathol 2003;163:2383–95.
29. Lasota J, Wozniak A, Kopczynski J, Dansonka-Mieszkowska A, Wasag B, Mitsuhashi T, et al. Loss of heterozygosity on chromosome 22q in

gastrointestinal stromal tumors (GISTs): a study on 50 cases. Lab Invest 2005;85:237–47.
30. Schofield DE, Beckwith JB, Sklar J. Loss of heterozygosity at chromosome regions 22q11-12 and 11p15.5 in renal rhabdoid tumors. Genes Chromosomes Cancer 1996;15:10–7.
31. Akagi K, Kurahashi H, Arita N, Hayakawa T, Monden M, Mori T, et al. Deletion mapping of the long arm of chromosome 22 in human meningiomas. Int J Cancer 1995;60:178–82.
32. Hartmann C, Nümann A, Mueller W, Holtkamp N, Simon M, von Deimling A. Fine mapping of chromosome 22q tumor suppressor gene candidate regions in astrocytoma. Int J Cancer 2004;108:839–44.
33. Castells A, Gusella JF, Ramesh V, Rustgi AK. A region of deletion on chromosome 22q13 is common to human breast and colorectal cancers. Cancer Res 2000;60:2836–9.
34. Su JL, Chen PS, Johansson G, Kuo ML. Function and regulation of let-7 family microRNAs. Microrna 2012;1:34–9.
35. Roush S, Slack FJ. The let-7 family of microRNAs. Trends Cell Biol 2008;18:505–16.
36. Tzatsos A, Paskaleva P, Lymperi S, Contino G, Stoykova S, Chen Z, et al. Lysine-specific demethylase 2B (KDM2B)-let-7-enhancer of zester homolog 2 (EZH2) pathway regulates cell cycle progression and senescence in primary cells. J Biol Chem 2011;286:33061–9.
37. Völkel P, Dupret B, Le Bourhis X, Angrand PO. Diverse involvement of EZH2 in cancer epigenetics. Am J Transl Res 2015;7:175–93.
38. Deb G, Singh AK, Gupta S. EZH2: not EZHY (easy) to deal. Mol Cancer Res 2014;12:639–53.
39. Pádua Alves C, Fonseca AS, Muys BR, de Barros E Lima Bueno R, Bürger MC, de Souza JE, et al. The lincRNA Hotair is required for epithelial-to-mesenchymal transition and stemness maintenance of cancer cell lines. Stem Cells 2013;31:2827–32.
40. Gupta RA, Shah N, Wang KC, Kim J, Horlings HM, Wong DJ, et al. Long non-coding RNA HOTAIR reprograms chromatin state to promote cancer metastasis. Nature 2010;464:1071–6.
41. Matouk IJ, Raveh E, Abu-lail R, Mezan S, Gilon M, Gershtain E, et al. Oncofetal H19 RNA promotes tumor metastasis. Biochim Biophys Acta 2014;1843:1414–26.
42. Lim J, Poulin NM, Nielsen TO. New strategies in sarcoma: linking genomic and immunotherapy approaches to molecular subtype. Clin Cancer Res 2015;21:4753–9.
43. Wilson BG, Roberts CW. SWI/SNF nucleosome remodellers and cancer. Nat Rev Cancer 2011;11:481–92.
44. Sherr CJ. The Pezcoller lecture: cancer cell cycles revisited. Cancer Res 2000;60:3689–95.
45. Eilers G, Czaplinski JT, Mayeda M, Bahri N, Tao D, Zhu M, et al. CDKN2A/p16 loss implicates CDK4 as a therapeutic target in imatinib-resistant dermatofibrosarcoma protuberans. Mol Cancer Ther 2015;14:1346–53.
46. Purkait S, Sharma V, Jha P, Sharma MC, Suri V, Suri A, et al. EZH2 expression in gliomas: correlation with CDKN2A gene deletion/ p16 loss and MIB-1 proliferation index. Neuropathology 2015;35:421–31.

Published OnlineFirst June 2, 2016; DOI: 10.1158/1541-7786.MCR-16-0068

Molecular Cancer Research

Evolution of Dermatofibrosarcoma Protuberans to DFSP-Derived Fibrosarcoma: An Event Marked by Epithelial–Mesenchymal Transition–like Process and 22q Loss

Silvia Stacchiotti, Annalisa Astolfi, Alessandro Gronchi, et al.

Mol Cancer Res 2016;14:820-829. Published OnlineFirst June 2, 2016.